BIOCHIP JOURNAL, Vol. 3, No. 2, 143-150, June 2009

Anti-biofouling Coating by Wrinkled, Dual-roughness Structures of Diamond-like Carbon (DLC)

Yudi Rahmawan[1,2], Kyung-Jin Jang[1], Myoung-Woon Moon[2], Kwang-Ryeol Lee[2] & Kahp-Yang Suh[1]

[1]School of Mechanical and Aerospace Engineering and the Institute of Advanced Machinery and Design, Seoul National University, Seoul 151-742, Korea
[2]Convergence Technology Laboratory, Korea Institute of Science and Technology, Seoul 130-650, Korea
Correspondence and requests for materials should be addressed to M.-W. Moon (mwmoon@kist.re.kr) and K.-Y. Suh (sky4u@snu.ac.kr)

Accepted 6 May 2009

Abstract

The textured surface with superhydrophobic nature was explored for an anti-biofouling template. Hierarchical structures composed of the nano-scale wrinkle covering on micro-scale polymer pillar patterns were fabricated by combining the deposition of a thin coating layer of biocompatible diamond-like carbon (DLC) and the replica molding of poly-(dimethylsiloxane) (PDMS) micro-pillars. The as-prepared surfaces were shown to have extreme hydrophobicity (static contact angle＞160°) owing to low surface energy (24.2 mN/m) and dual-roughness structures of the DLC coating. It was explored that the hierarchical surfaces showed poor adhesion of the Calf Pulmonary Artery Endothelial (CPAE) cells for cultures of 7 days suggesting that the 3-dimensional (3-D) patterned superhydrophobic DLC coating exhibits excellent anti-biofouling properties against non-specific cell adhesion. In particular, the reduced filopodia extension during cell growth was caused by disconnected focal adhesions on the pillar pattern. This limited cell adhesion could prevent undesired growth and proliferation of biological species on the surface of biomedical devices such as stents, implants or even injection syringes.

Keywords: Diamond-Like Carbon (DLC), Cell adhesion, Superhydrophobicity, Dual-scale structure, Anti-biofouling

Introduction

The interaction behaviors between biological environment with solid surfaces have been extensively studied in recent years. In general, undesired biological attachment on engineered solid surface has produced severed problems in various fields, ranging from the macroscopic level such as microbiology-induced corrosion in marine structures and ships to the microscopic level such as malfunction of biomedical devices. The biofouling mechanism has involved a complex interplay between chemistry, surface morphology and polarity[1-3]. In biomedical field, the failure of some intravascular biomedical devices during operation is caused by proliferation of cells on such devices. This biofouling is accelerated by adherence of proteins, glycoproteins, or bacteria while the vascular flow is insufficient to clean the surface[4]. Particularly, the current restenosis rate of the implanted stent after one month is about 30-40% due to the proliferation of cells and the resulting accumulation of sludge inside the stent[5,6]. Several methods have been developed to prevent cell proliferation on biomedical devices, such as radiotherapy[7,8], dietary program[9], and drug eluting surfaces[10]. While these methods are useful, there are potential drawbacks involving complexity of fabrication and operation[11]. Therefore, it is of great importance to develop a device with self-cleaning and anti-biofouling characteristics, together with long-term stability, in *in-vivo* environments.

Recently, surface texturing to improve superhydrophobicity has been extensively studied both experimentaly and theoretically[12-14]. Furthermore to fabricate a water-repellent superhydrophobic surface, it can be desirable to combine the methods of top-down and bottom-up processes, which has also been demonstrated using vertically aligned carbon nanotubes[15,16], porous membranes[17], or micelle aggregation[18]. Among the fabrication methods reported so far, however, superhydrophobic surfaces with biocompatibility-an essential aspect of biomedical applications-have been relatively unexplored. The use of traditional engineering materials for nano and microfabrication, such as silicon, metals, or non-biocompatible polymers, in biomedical applications, may result in degradation of such materials and consequently improper functionality on cellular and systemic activities under the host environment[19]. Therefore, use of biocompatible materials for surface finishing is necessary for long-term stability of the system.

In this work, we explore the potential of surface textures coated with a material of low surface energy as

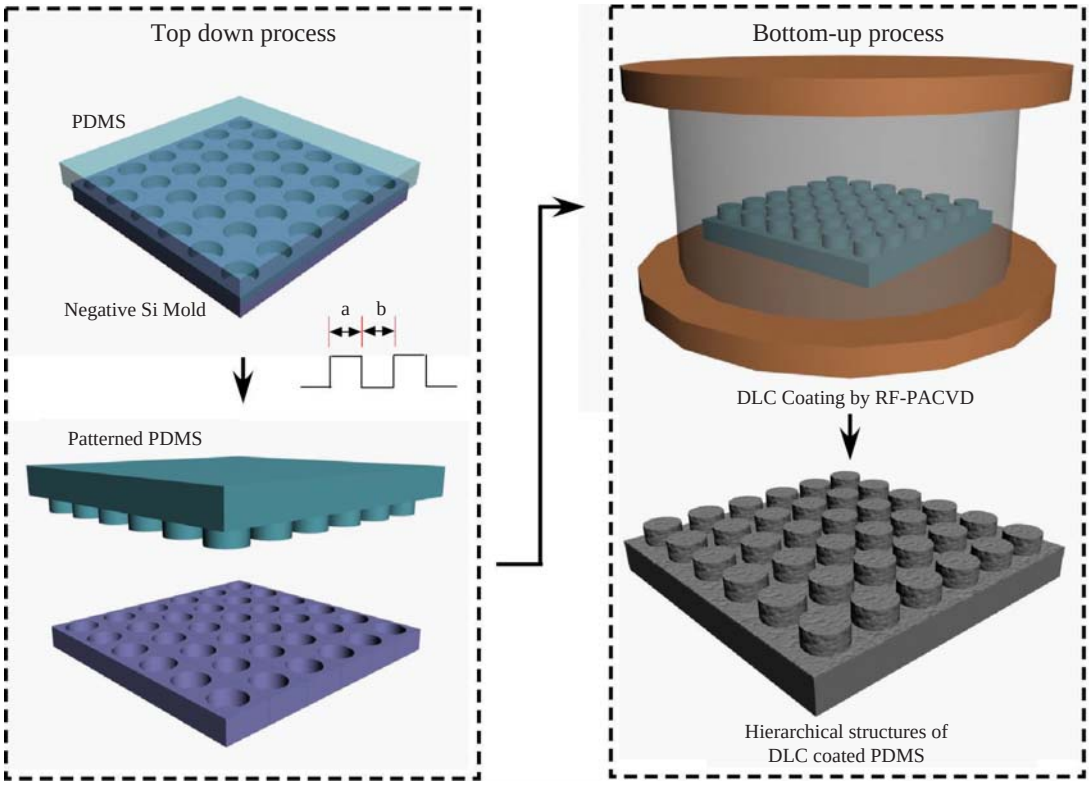

Figure 1. A schematic diagram of the fabrication procedure for dual-roughness DLC hierarchical structures. 'a' and 'b' inserted in the schematic of top-down process are denoted as the pillar diameter and pillar-pillar separation distance, respectively.

well as of biocompatibility as a means to prevent biofouling at cellular level. Hierarchical surfaces was fabricated with a nanoscale wrinkle formation of the diamond-like carbon (DLC) coating on a micro-scale patterns by soft-lithographic method as shown in Figures 1 and 2. DLC coating was chosen for surface finishing layer due to its superior tribological and mechanical properties as well as chemical inertness in biological environment with biocompatibility and hemocompatibility[20-22]. Futhermore, poly-(dimethylsiloxane) (PDMS) is a powerful material for building micro- and nanostructures with the vast advantages of soft lithography to provide a convenient, effective, and low-cost method for many biological assays application[23,24]. A Non-linear wrinkle pattern can be formed in DLC film on soft polymer such as PDMS, which is caused by the difference in elastic properties between DLC film and polymer and the high compressive stress in DLC film[25]. The 3-dimensional (3-D) patterned, hierarchical-roughness structures are used as an anti-biofouling coating to resist cell adhesion using bovine endothelial cells. The experimental results revealed that the adhesion and proliferation of CPAE cells is highly restricted on such superhydrophobic surfaces when the spacing between micro-pillars is smaller than the diameter of the cells. In addition, the effects of various micro-pillar spacing ratios on the interplay between superhydrophobicity and cell adhesion are investigated as described below.

Results and Discussion

A schematic illustration of the fabrication procedure of the dual-roughness DLC structure with combining both top-down and bottom-up processes shown in Figure 1. For the top-down process, direct replica molding of PDMS from a silicon master was used to produce micrometer scale pillars of 4 μm diameter and 5 μm height, separated in equally spaced square array. Specimens of ten different inter-pillar gap distances were tested for the wetting and bio-adhesion experiments, with ten different integer values of spacing ratio ranging from 1 to 10. The spacing ratio is defined as the ratio of the nearest pillar-pillar separation distance to the pillar diameter (shown as b/a in Figure 1). To fabricate nanostructures on the micro-pillar surface structures, a bottom-up process was ado-

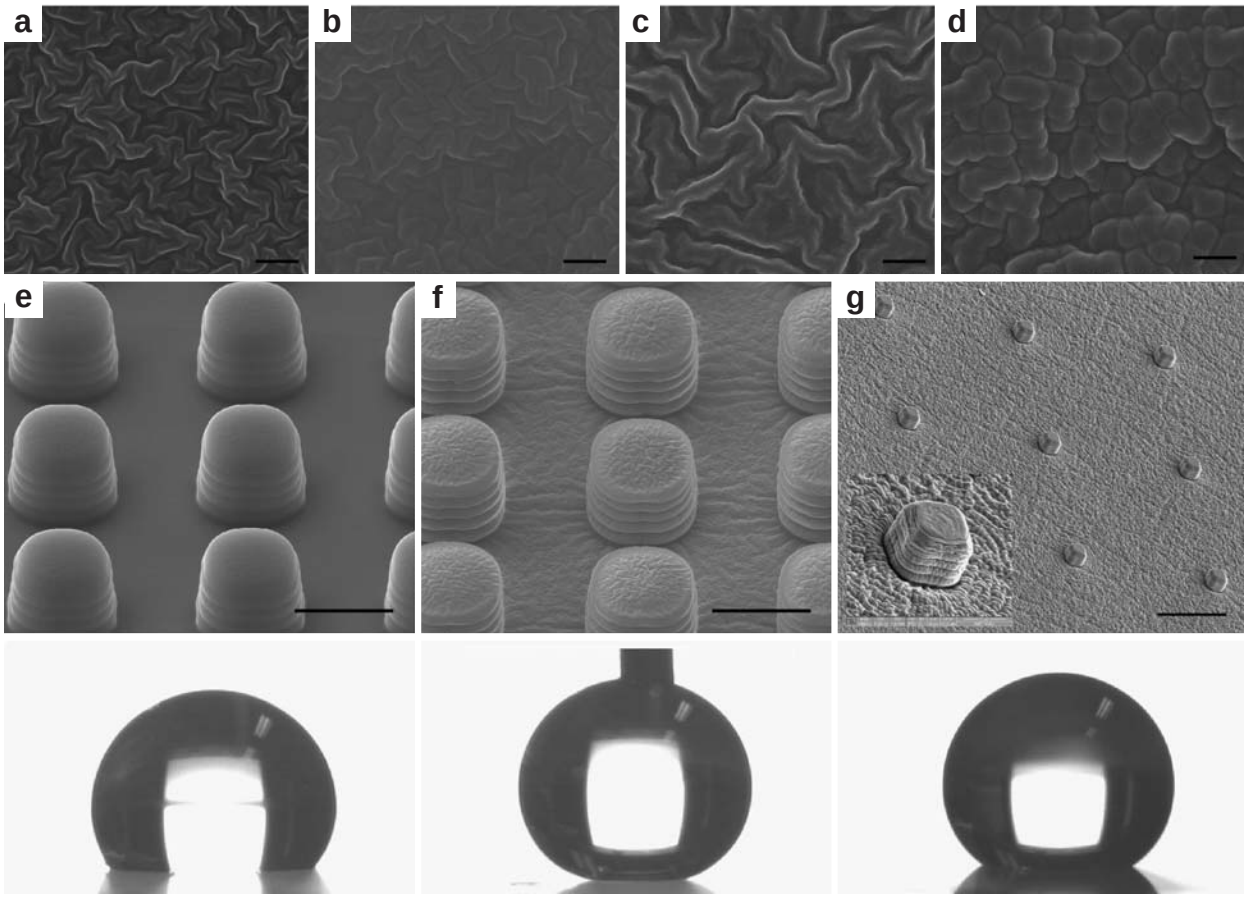

Figure 2. SEM images of patterned PDMS by DLC coating. Wrinkle evolution is observed after DLC coating for 10 s (a), 30 s (b), 1 m (c), 10 m (d). The micropatterned of PDMS before (e) and after (f) DLC coating is shown. The picture in (g) shows a large area view along with a magnified view in the inset. Contact angles of water droplet show that the surface is highly water-repelling after DLC coating (contact angle ~160° in (f)). Scale bars are 500 nm in Figure 2 (a-d), 5 μm in Figure 2 (e, f) and 20 μm in Figure 2 (g).

pted by using a radio frequency-plasma assisted chemical vapour deposition (RF-PACVD) of DLC films from hexametyldisiloxane (HMDSO) monomer as a precursor. HMDSO was selected due to its very low surface energy (24.2 mN/ m) close to that of poly-(tetrafluoroethylene) (PTFE) (18.5 mN/m)[26].

As shown in Figure 2, random orientation of a highly contorted hierarchical wrinkle structure is clearly seen after deposition of a DLC thin film on pre-patterned pillars of PDMS. For the deposition for 10 s, an isotropic wrinkle pattern was formed on the top as well as on the bottom valley surfaces of the pillars. With increasing deposition time to 1 min, a dual-mode wavy structure with the primary mode of ~1.1 μm and the secondary mode of ~120 nm appeared. Based on these results, an optimum deposition condition for superhydrophobicity was obtained[25]: deposition time of 30 s and base and deposition pressures of 0.01 and 10 mTorr, respectively, at a bias voltage (V) of -400 V. This process condition allows for a distinct hierarchical structure with microscale PDMS pillars covered with a uniform nanoscale DLC coating. For the optimum condition of nanoscale wrinkle formation on microscale pillars, it has been shown theoretically and experimentally that the spacing ratio of 1 to 4 gives superhydrophobicity properties on the surfaces as described in our previous work[25].

Recent studies have shown that there are strong correlations between cell adhesion and the distribution of extra cellular matrix (ECM) proteins[27-29], surface geometrical features[30,31], and surface free energy[32,33]. Our primary interest is to potentially apply the superhydrophobic surfaces to implanted biomedical devices. To this end, we first need to examine the cell adhesion on superhydrophobic surfaces for a prolonged period of time. We believe that the superhydrophobic surfaces would lower the adhesion strength of the cells, due to the limited contact between the cell medium and the

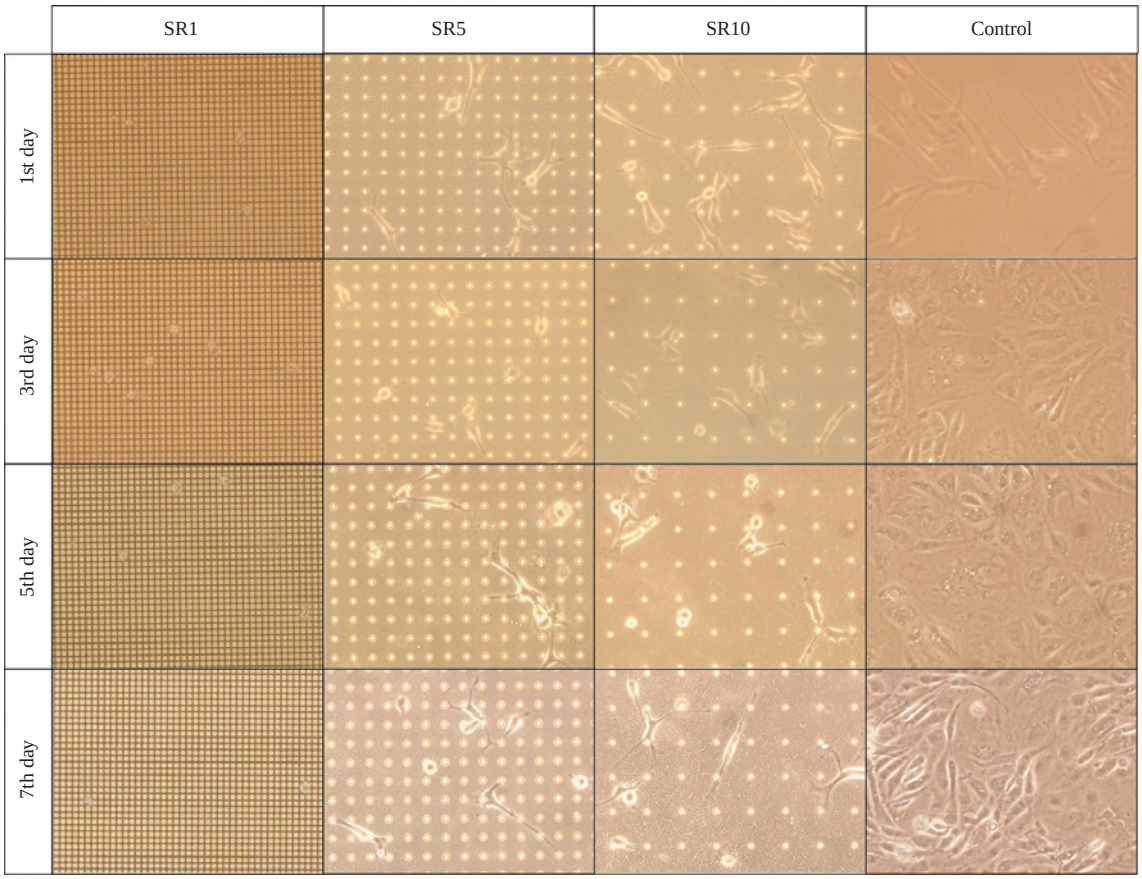

Figure 3. The optical microscope images of CPAE cells cultured over 7 days on hierarchically structured surfaces with different spacing ratios of micro-pillars (1, 5, and 10). Cells were also cultured on the petri dish as control. Surfaces of the spacing ratio of micro-pillars of 1 showed the least cell attachment compared to those of 5 and 10 and the control.

substrate. The initial cell attachment is restricted by less ECM proteins adsorbed on the surface, in which the initial superhydrophobicity plays a key role. As time goes by, the cell attachment can be enhanced as the cells recognize the surface by secreting their own ECM proteins or as the surface loses its original hydrophobicity. Nonetheless, the cell proliferation would be highly restricted on the hierarchical structures in that the focal adhesions are only formed at the peak of nanoscale wrinkles, while these adhered cells have difficulty in crawling into the spaces between micropillars. From a surface free energy point of view, cell adhesion is driven by the balance between dispersive and polar components of the total surface energy. Baier *et al.*[32] reported that cell adhesion could be minimal when surface free energy is between 20 to 30 mN/m, which is very close to that of the DLC coating (24.2 mN/m) used in our experiments.

Figure 3 shows the adhesion behavior of CPAE cells on surfaces with different degrees of hydrophobicity when cultured over 7 days. On hierarchical structures with the spacing ratio of 1 to 4 (superhydrophobic surfaces), the cells remained less spread-out with a spherical shape after cultures of several days. The cell density was $< \sim 50$ cells/mm^2 even for a culture period of 1 week, which was smaller than that on the Petri dish control by one order of magnitude. As mentioned above, we attribute the reduction in the initial cell attachment on superhydrophobic surfaces to the reduced amount of ECM proteins. In addition, the cells cannot easily crawl into the spaces between micropillars, yielding suspended cell attachment and limited cell proliferations.

When the micropillar spacing is larger than the diameter of cells (10-20 μm), i.e., spacing ratio > 4, the attachment and growth of cells becomes distinctively larger, since the cells can crawl in between the larger micropillar spaces and anchor themselves to the bottom surface. As shown in Figure 3, the cells were relatively well spread with many interconnections for the spacing ratio of 5 and 10. On the petri dish surface (control), the cells formed a confluent layer within a

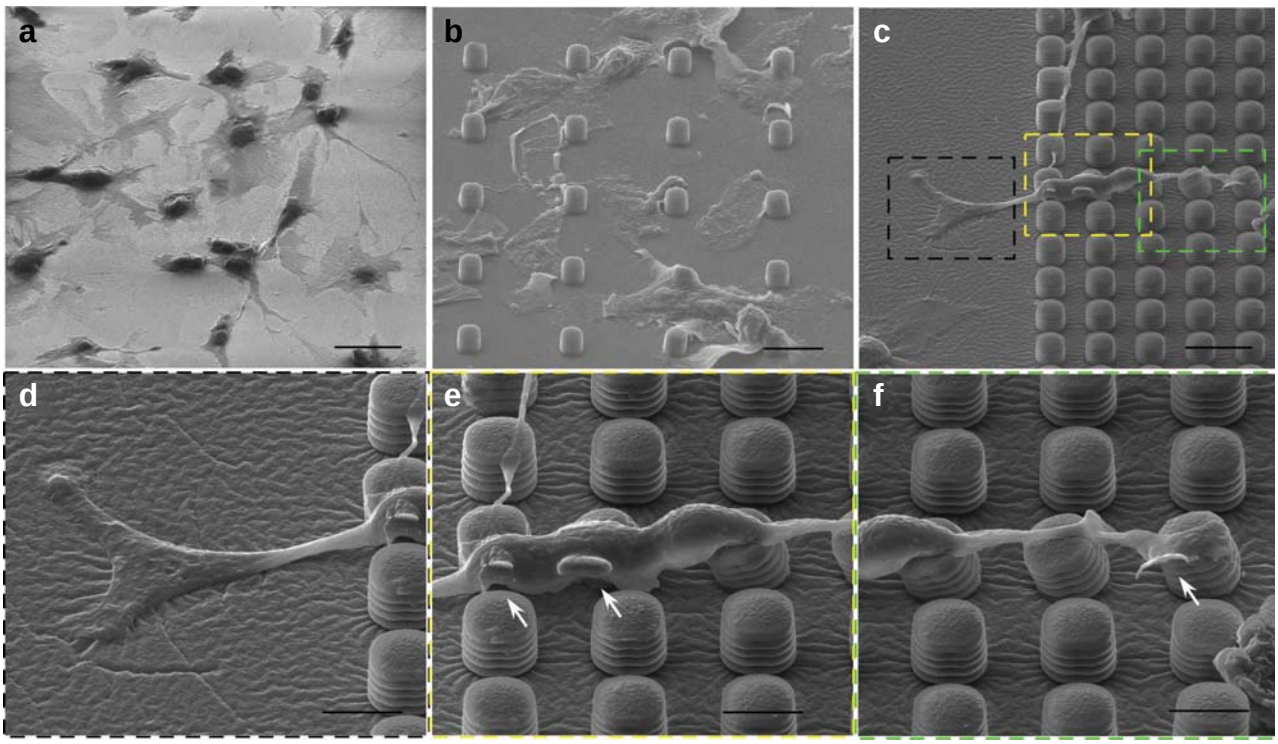

Figure 4. Adhesion behavior of CPAE cells on: (a) flat PDMS, (b) hierarchical wrinkled structure with high spacing ratio of 5 (hydrophobic), (c) hierarchical wrinkled structure with low spacing ratio of 1 (superhydrophobic), (d-f) details of cell morphology on the surfaces shown in Figure 5c. Arrows indicate the detachment of filopodia of CPAE cells from wrinkled pillar surfaces. Scale bars are 10 μm (Figure 4a-c) and 5 μm (Figure 4d-f).

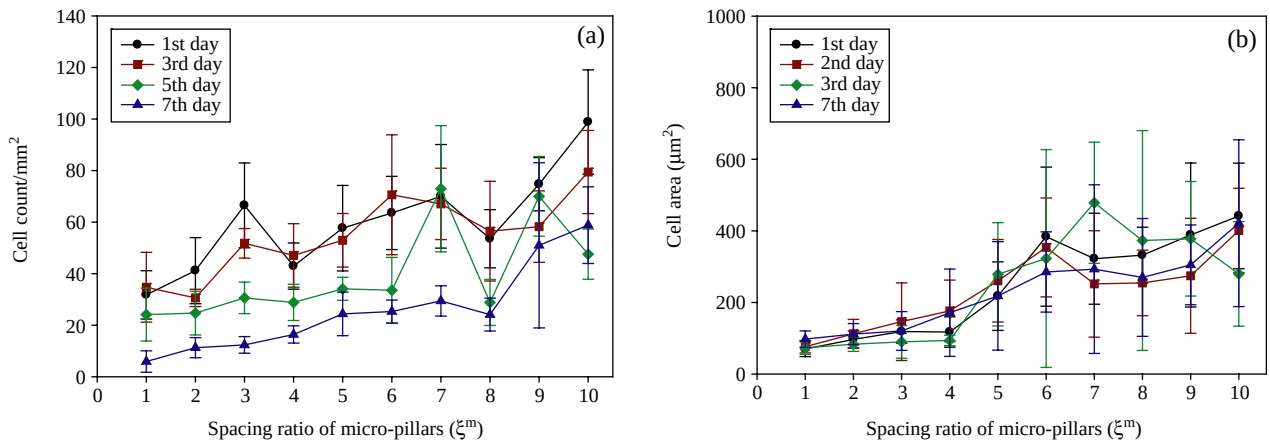

Figure 5. Adhesion behavior of CPAE cells on surfaces with different degree of hydrophobicity when cultured over 7 days. The cell density (a) and the area (b) are shown as a function of spacing ratio, where samples with spacing ratio of 1 to 4 show superhydrophobic surfaces.

week. The details of cell morphology on the surfaces with different hydrophobicity are shown in Figure 4. It is clearly seen that CPAE cells were trying to make a confluent layer on the flat surface (Figure 4a). As the hydrophobicity increased by the application of micro- and nanoscale roughness, cells were more difficult to spread onto the surfaces. Finally on the surfaces in the superhydrophobic regions (hierarchical

wrinkle structures with spacing ratio of micro-pillars from 1 to 4 shown in Figure 4c), cells were not able to penetrate into the micro-pillars space. Therefore a very weak focal point adhesion was created only on the summit of the nanoscale wrinkle structures. Consequently, some of the focal adhesion points were detached from the surface (see arrows in Figure 4e, f).

Figure 5a shows the measurement of cell density on surfaces with different hydrophobicity. We observed that the dual-roughness DLC coating can resist against cell adhesion without significant increase in cell density on hierarchical surfaces with the spacing ratio of 1 to 4. Interestingly, as the culture period increased, the cell density in most samples decreased due to the larger population of dead cells. In contrast, for the petri dish control surface, cells were well spread-out, creating a confluent layer within a week. To elaborate on cell morphology and growth on the hierarchical structures, we measured the cell spreading area as a function of hydrophobicity (or spacing ratio) as shown in Figure 5b. Regardless of the culture period, the cell spreading area significantly increased on moderate hydrophobic surfaces (spacing ratio higher than 4). This result supports our hypothesis that the limited contact between the cell medium and the substrate gives rise to poor cell adhesions on superhydrophobic surfaces. These experimental observations therefore suggest that the superhydrophobic, dual-roughness surface in our study could act as an anti-biofouling coating against cell adhesion.

Conclusions

We have presented dual-roughness, hierarchical structures of DLC as an anti-biofouling coating against non-specific adhesion of CPAE cells. The structures were fabricated by depositing a thin coating layer of biocompatible DLC on PDMS micro-pillars created from replica molding. Our experimental found that superhydrophobicity could be achieved on the 3-D hierarchical surface structure with a low microstructure spacing ratio of 1 to 4. The adhesion assays on surfaces with different degree of hydrophobicity revealed that the proliferation of CPAE cells was highly restricted on superhydrophobic surfaces with the spacing smaller than the diameter of the cells; the limited spacing restricts the entry of the cell, resulting in suspended cell attachment and limited growth. The low surface free energy of DLC coating further contributed to the reduced adhesion and growth of the cells.

The simple fabrication method presented here provides an effective way of creating 3-D hierarchically structures with superhydrophobicity and anti-biofouling. These properties would be particularly useful for biomedical devices such as stents, implants or even injection syringes.

Materials and Methods

Preparation of Dual-roughness Structures of DLC

Details on the preparation of dual-scale DLC structures can be found elsewhere[25]. Briefly, PDMS (Sylgard 184 Silicon elastomer, Dow Corning) was used as the soft base material (Young's modulus of PDMS ~20 MPa). To make pillar structures with different spacing ratio, the standard soft lithographic technique called replica molding was used. The array of micropillars with spacing ratio from 1 to 10 was replicated from 4 inch diameter of silicon master. Each array had $1 \times 1\ cm^2$ area, containing 4 μm diameter and 5 μm height of micropillars. To generate nanometer scale wrinkle structures, RF-PACVD was used to deposit a very thin layer of DLC on pre-patterned PDMS surfaces. The precursor gas of hexamethyldisiloxane (HMDSO) was decomposed into a DLC film at a base pressure and a deposition pressure of 10^{-6} and 10^{-2} Torr, respectively.

Contact Angle (CA) and Contact Angle Hysteresis (CAH) Measurements

Deionized (DI) water with a droplet volume set at 5 μL was used in the measurement of static CA with sessile droplet mode. For CAH measurement, advancing and receding CAs were measured when a water droplet with total volume of about 50 μL was drawn in and out to the surfaces. The data was averaged over at least 5 different locations using a contact angle analyzer (KRUSS DSA 100).

Cell Culture and Viability Test

Calf pulmonary artery endothelial (CPAE) cells were purchased from the American Type Culture Collection (ATCC) and cultured on the surfaces with hierarchical structures. The surfaces were cleaned by 70% ethanol, DI water and phospate-buffered saline (PBS) (pH 7.4) at room temperature. CPAE cells were then seeded at a cell density of 1.5×10^5 cell/mL and maintained with the culture medium (Dulbecco's modified Eagles medium/DMEM, 10% fetal bovine serum, and 1% penicillin-streptomycin) at 37°C in a humidified 5% CO_2 incubator. For measuring cell morphology, the cells were incubated with calcein-AM (2 μM, green fluorescence) in PBS at 37°C in humidified 5% CO_2 incubator. The cells were washed in PBS and immediately viewed with an optical inverted microscope (Olympus

IX71) equipped with a reflected light fluorescence unit.

Observation

The details of hierarchical structures and cells morphology were observed under a scanning electron microscope (SEM) (NanoSEM 200, FEI company). Prior to SEM observation, the cells were dehydrated using multistage ethanol solutions (30, 50, 80 and 99 %) after paraformaldehyde (PFA, 4% in PBS) incubation for 15 min. The cells were then fixed using hexamethyldisilazane (HMDS) for 30 min. 10 nm Pt layer was deposited using a vapor deposition method for preventing the electron charging during SEM observation with the accelerating voltage of 5 kV.

Acknowledgements

This work was supported by Korea Science and Engineering Foundation (KOSEF) grant funded by the Korea government (MOST) (R01-2007-000-20675-0), the Micro Thermal System Research Center of Seoul National University, and the Korea Research Foundation Grant funded by the Korean Government (MOEHRD) (Grant KRF-J03003). This work was supported in part by a grant (06K1501-01610) from the CNMT under the '21st Century Frontier R & D Programs' of MEST of Korea (MWM, KRL).

References

1. Mrksich, M. & Whitesides, G.M. Using self-assembled monolayers to understand the interactions of man-made surfaces with proteins and cells. *Annu. Rev. Biophys. Biomol. Struct.* **25**, 55-78 (1996).
2. Genzer, J. & Marmur, A. Biological and synthetic self-cleaning surfaces. *MRS Bulletin* **33**, 742-746 (2008).
3. Chung, S.H. & Min, J. A microscopic investigation on the effect of hydrophobic properties on cell adhesion on a PDMS surface. *Biochip J.* **2**, 141-147 (2008).
4. Seitz, U. *et al.* Biliary stent clogging solved by nanotechnology? In vitro study of inorganic-organic sol-gel coatings for teflon stents. *Gastroenterology* **133**, 65-71 (2007).
5. Fischman, D.L. *et al.* A randomized comparison of coronary-stent placement and balloon angioplasty in the treatment of coronary-artery disease. *New Engl. J. Med.* **331**, 496-501 (1994).
6. Serruys, P.W. *et al.* A comparison of balloon-expandable-stent implantation with balloon angioplasty in patients with coronary-artery disease. *New Engl. J. Med.* **331**, 489-495 (1994).
7. King, S.B. *et al.* Endovascular beta-radiation to reduce restenosis after coronary balloon angioplasty-Results of the beta energy restenosis trial (BERT). *Circulation* **97**, 2025-2030 (1998).
8. Raizner, A.E. *et al.* Inhibition of restenosis with beta-emitting radiotherapy-Report of the proliferation reduction with vascular energy trial (PREVENT). *Circulation* **102**, 951-958 (2000).
9. Wang, C.C. *et al.* n-3 fatty acids from fish or fish-oil supplements, but not alpha-linolenic acid, benefit cardiovascular disease outcomes in primary- and secondary-prevention studies: a systematic review. *Am. J. Clin. Nutr.* **84**, 5-17 (2006).
10. Hehrlein, C., Arab, A. & Bode, C. Drug-eluting stent: the "magic bullet" for prevention of restenosis? *Basic Res. Cardiol.* **97**, 417-423 (2002).
11. van der Hoeven, B.L. *et al.* Drug-eluting stents: results, promises and problems. *Int. J. Cardiol.* **99**, 9-17 (2005).
12. Neinhuis, C. & Barthlott, W. Characterization and distribution of water-repellent, self-cleaning plant surfaces. *Ann. Bot-London* **79**, 667-677 (1997).
13. He, B., Patankar, N.A. & Lee, J. Multiple equilibrium droplet shapes and design criterion for rough hydrophobic surfaces. *Langmuir* **19**, 4999-5003 (2003).
14. Quere, D. Non-sticking drops. *Rep. Prog. Phys.* **68**, 2495-2532 (2005).
15. Lau, K.K.S. *et al.* Superhydrophobic carbon nanotube forests. *Nano Lett.* **3**, 1701-1705 (2003).
16. Li, S.H. *et al.* Super-hydrophobicity of large-area honeycomb-like aligned carbon nanotubes. *J. Phys. Chem. B.* **106**, 9274-9276 (2002).
17. Erbil, H.Y., Demirel, A.L., Avci, Y. & Mert, O. Transformation of a simple plastic into a superhydrophobic surface. *Science* **299**, 1377-1380 (2003).
18. Xie, Q.D. *et al.* Facile creation of a bionic super-hydrophobic block copolymer surface. *Adv. Mater.* **16**, 1830-1833 (2004).
19. Williams, D.F. On the mechanisms of biocompatibility. *Biomaterials* **29**, 2941-2953 (2008).
20. Robertson, J. Diamond-like amorphous carbon. *Mat. Sci. Eng. R.* **37**, 129-281 (2002).
21. Roy, R.K. & Lee, K.R. Biomedical applications of diamond-like carbon coatings: A review. *J. Biomed. Mater. Res. B.* **83B**, 72-84 (2007).
22. Peng, X.L. & Clyne, T.W. Mechanical stability of DLC films on metallic substrates: Part I-film structure and residual stress levels. *Thin Solid Films* **312**, 207-218 (1998).
23. Kim, P.N. *et al.* Soft lithography for microfluidics: a review. *Biochip J.* **2**, 1-11 (2008).
24. Choi, H.G. *et al.* Fabrication of nanopattern by nano-imprint lithography for the application to protein chip. *Biochip J.* **3**, 76-81 (2009).
25. Rahmawan, Y., Moon, M.-W., Kim, K.-S., Lee, K.-R. & Suh, K.-Y. Wrinkled, dual-scale structures of diamond-like carbon (DLC) for superhydrophobicity. Submitted (2009).
26. Grischke, M., Hieke, A., Morgenweck, F. & Dimigen, H. Variation of the wettability of DLC-coatings by network modification using silicon and oxygen. *Diam.*

Relat. Mater. **7**, 454-458 (1998).
27. Chen, C.S., Mrksich, M., Huang, S., Whitesides, G. M. & Ingber, D.E. Geometric control of cell life and death. *Science* **276**, 1425-1428 (1997).
28. Giancotti, F.G. & Ruoslahti, E. Transduction-Integrin signaling. *Science* **285**, 1028-1032 (1999).
29. Kane, R.S., Takayama, S., Ostuni, E., Ingber, D.E. & Whitesides, G.M. Patterning proteins and cells using soft lithography. *Biomaterials* **20**, 2363-2376 (1999).
30. Brock, A. *et al.* Geometric determinants of directional cell motility revealed using microcontact printing. *Langmuir* **19**, 1611-1617 (2003).
31. Kim, H.J., Ryu, J.C. & Oh, S.J. Protein interactions on nano-scale controlled surface. *Biochip J.* **3**, 71-75 (2009).
32. Baier, R.E., Depalma, V.A., Goupil, D.W. & Cohen, E. Human-platelet spreading on substrata of known surface-chemistry. *J. Biomed. Mater. Res.* **19**, 1157-1167 (1985).
33. Zhao, Q. Effect of surface free energy of graded NI-P-PTFE coatings on bacterial adhesion. *Surf. Coat. Tech.* **185**, 199-204 (2004).